DOI: 10.71762/2967-8504

Research Paper

Investigation of Steel Slabs Marker Robotic Arm Control Parameters in Noise and Disturbance Absence/Presence

Mohammad Sajjad Mahdieh[1*]

[1]Department of Mechanical Engineering, Shahid Chamran University of Ahvaz, Ahvaz, Iran

[*]Email of the Corresponding Author: s.mahdieh@scu.ac.ir

Received: August 31, 2024; Accepted: October 17, 2024

Abstract

At Mobarakeh Steel Company, the writing on steel slabs is currently performed by manual labor, which has several negative consequences. To address this issue, a project has been initiated to implement robots instead. A robotic arm with five degrees of freedom (three related to the arm and two related to the wrist) has been developed to write letters and numbers on the steel slabs. This article details the design, dynamics, and control of the robotic arm. The dynamics were solved using the Newton-Euler method, while the robot's control was calculated using the computed torque method. Additionally, the robustness of the designed controller against noise and disturbances was evaluated. The effectiveness of the controller's performance was demonstrated through simulations. Furthermore, the robot's path was examined to ensure it did not cross any singular points. The results indicated that the robot's passage through its singular point was monitored, and it was confirmed that the robot did not cross the singular point.

Keywords

Marker Robot, Steel Slabs, Robot Dynamics, Robot Control

1. Introduction

In the steel industry of advanced countries, to write on steel slabs, they use marker robots to take advantage of its advantages such as high speed and accuracy and the elimination of human labor [1-6]. In 1979, Hollerbach was able to write by a humanoid robot. He and his group were able to design the first route for a writer's robot. What Hollerbach did at that time was very significant because his simple research later became the foundation of more serious industrial projects.

The humanoid robotic arm that he used for writing was a three-degree-of-freedom arm [7]. In 1991, Suh and his colleagues presented an efficient and optimal method for designing the path of paint-spraying robots. Optimizing the path of paint-spraying robots was a vital subject in the industry at that time because by optimizing the trajectory of paint-spraying robots, a significant amount of paint was saved, resulting in a significant saving in time and cost [8]. In 1994, Antonio conducted research on the design of the movement trajectory of a robot that covered different parts by spraying and obtained results. The research conducted by Antonio was the foundation of the next industrial projects

[9]. In 1997, Asakawa developed a new method of designing the trajectory of car body paint spraying robots. His method, which was implemented under the title of Teachingless robots, was successful and saved time and money for the Hyundai company [10]. In 1996, Hertling researched the design of complex and curved paths of the paint spraying robot. Of course, Hertling's work remained a research project, but his research was precious for subsequent research [11]. Many control parameters are related to the physical and mechanical properties of the robot. Therefore, applying precise manufacturing methods such as machining and forming processes, helps to obtain these parameters accurately [12-19]. There are several other surveys have been conducted on this issue some of which are introduced in the papers [20-25].

Currently, in the steel industries of our country, writing on the steel slabs is done by human power, which has its problems. Therefore, a project based on the design and manufacturing of such a robot was defined, and part of its results (design of the dynamics and control) are presented in this article. The marker robot draws letters and numbers on the steel slabs with an automatic spray gun (pistol). Due to the use of an automatic gun and the automatic ON and OFF of the paint spraying, there is no need to separate the gun from the slab. However, the path of the robot to write letters is defined continuously. Figure 1 shows a marker robot and automatic spray gun used in steel-making factories. In this article, the kinematic solution (direct and inverse) of the problem and how to design the trajectory are not presented, and only the results of graphic simulations are given. The purpose of this article is to design a suitable controller for the robot. For this purpose, after solving the kinematics of the problem, the dynamics of the robot should be checked. For the dynamic solution of the robot, parameters such as the mass of the members, the center of mass of the members, and so forth are needed. Therefore, the two issues of solving the dynamics and designing the robot should be performed simultaneously, the parameters needed to solve the dynamics of the robot should be obtained, and wherever it is necessary, the necessary changes should be made in the design parameters (however, how to design the robot and its details are not given in this article). Then, the dynamics of the robot are solved by the Euler-Newton method, and after solving the dynamics of the robot, the controller is designed. The robot is controlled by the computed torque method which is the usual method of controlling industrial robots. Finally, the robustness of the designed controller to disturbance and noise has been checked and its results have been presented. As mentioned, in the steel industries of our country, writing on the steel slabs is done by human force, which has its problems. This paper presents an innovative solution to apply a writer's robotic arm instead of the human force.

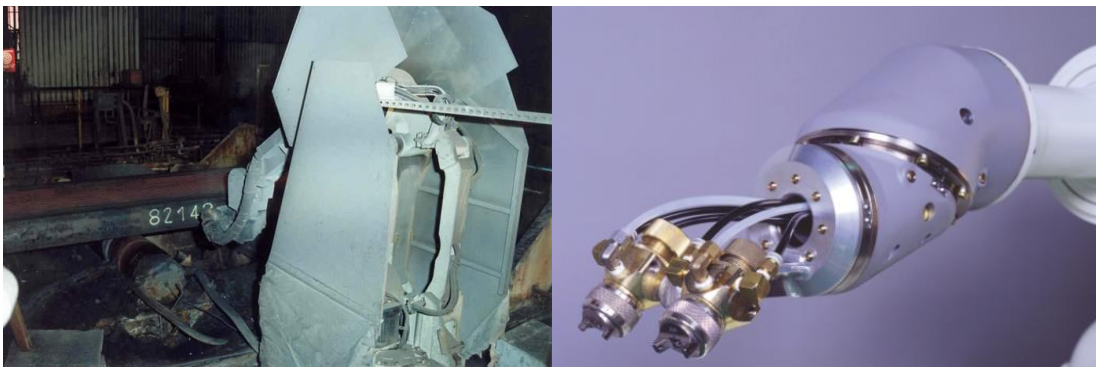

Figure 1. Marker robot and automatic spray gun

2. Research Method

2.1 Trajectory Planning of the Robot

To check the dynamics of the robot, the trajectory planning process must be determined first. It means that the motion equations of the path can be written in terms of space-time equations. For this, first, all the letters and numbers must be divided into their components, which are line segments or arcs. Therefore, a letter or number consists of a series of line segments or arcs. The final operator of the robot, by following these routes, can finally write the desired letter or number on the board. Figure 2 shows the designed marker robot for the present project. According to Figure 3, the letter F consists of six line segments, and the letter D consists of two line segments and one arc.

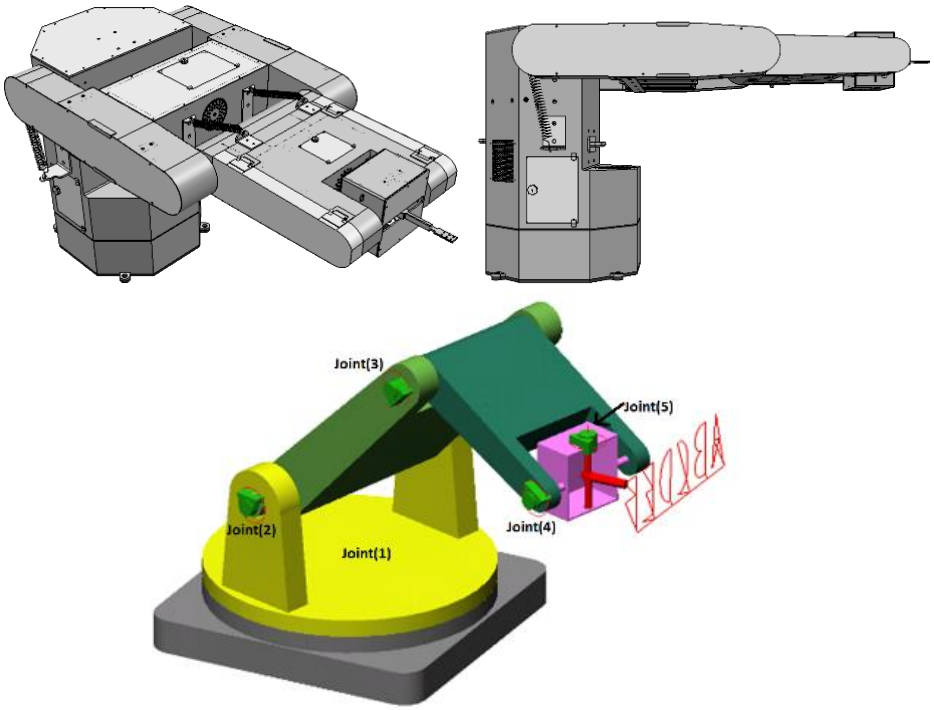

Figure 2. Designed marker robot

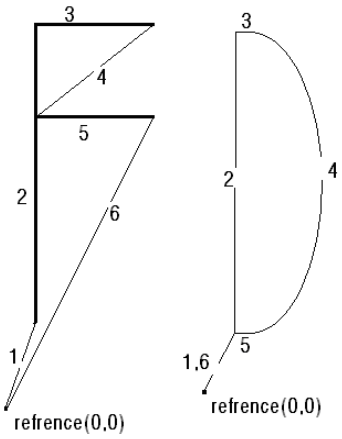

Figure 3. The path of the end-effector to write letters D and F

Now the equations of each component of a letter or number should be obtained in terms of time. It is assumed that the end-effector of the robot must travel a path that includes a line segment or a curve. For this, the final end-effector must start from zero speed with constant acceleration, continue with constant speed, and finally reach zero speed with negative acceleration. In this case, the speed-time diagram of the final robot operator for traversing lines and curves is shown in Figure 4.

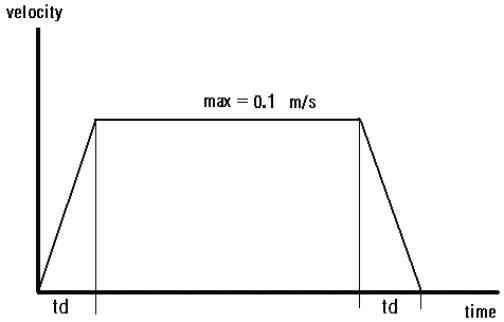

Figure 4. Velocity-time diagram of the robot's end-effector

td is the acceleration time (positive or negative) of the robot, and by applying *td*, the path of a line segment or curve is divided into three parts: two parts that the robot travels with acceleration (positive or negative) and one part that the robot travels with constant speed. For example, the equations of a line segment are according to relations 1:

$$\begin{cases} l_1 = \frac{1}{2}960t^2 \\ 0 \le t \le 0.1 \end{cases} \quad \begin{cases} l_2 = 96t - 4.8 \\ 0.1 \le t \le 0.93 \end{cases} \quad \begin{cases} l_3 = -\frac{1}{2}960t^2 + 988.8t - 419.925 \\ 0.93 \le t \le 1.03 \end{cases} \tag{1}$$

The end-effector starts moving from zero speed with increasing acceleration at the origin and after traveling the segment L_1, it travels the segment L_2 at a constant speed and finally travels the segment L_3 with decreasing acceleration to reach the destination point. At the destination point, the speed of the final conductor is zero.

2.2 Robot dynamics

As mentioned, after obtaining the equations of the path in terms of time, the dynamic equations of the robot can be obtained from the Newton-Euler method. The equations of motion in the Newton-Euler method are based on the force balance between the robot members. The complete algorithm for calculating joint torques using joint movement consists of two parts. In the first part, the velocities and accelerations of members are calculated from member *1* to member *n* using repeated relations, and Newton-Euler equations are written for each member. In the second part, the forces and moments between the members and the driving moments of the joints are calculated sequentially from member *n* to member 1 [26]. According to the Newton-Euler relations, the diagram of torques of joints 2 and *3* of the robot to draw a line segment is calculated in MATLAB and Simulink software and is given in Figures 5 and 6 (torques are in Newton-meters).

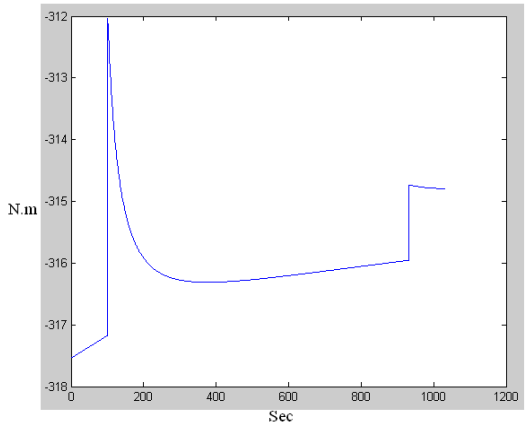

Figure 5. Diagram of the moment entering into joint 2

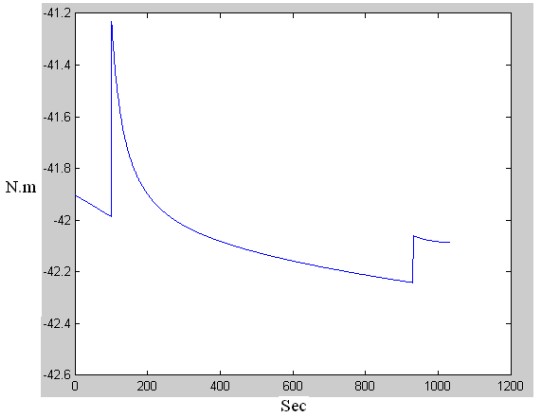

Figure 6. Diagram of torque entering into joint 3

2.3. Robot Control

In this article, the robot is controlled using the Computed Torque Method, CTM, by using PID in the outer loop. CTM method or control through computed torque is one of the common methods of robot control. Many industrial robots use PD or PID, so this type of controller has been applied in this project. In PID control or proportional-derivative-integrator control, 2 relations prevail [27]:

$$\begin{aligned}
&\dot{\varepsilon} = e \\
&u = -K_V\dot{e} - K_P e - K_i\varepsilon \\
&\tau = M(q)\ddot{q}_d + K_V\dot{e} + K_P e + K_i\varepsilon) + N(q,\dot{q}) \\
&\frac{d}{dt}\begin{bmatrix}\varepsilon\\ e\\ \dot{e}\end{bmatrix} = \begin{bmatrix}0 & I & 0\\ 0 & 0 & I\\ -K_i & -K_P & -K_V\end{bmatrix}\begin{bmatrix}\varepsilon\\ e\\ \dot{e}\end{bmatrix} + \begin{bmatrix}0\\ 0\\ I\end{bmatrix}w \\
&\Delta_c(s) = |s^3 I + K_V s^2 + K_P s + K_i|
\end{aligned} \tag{2}$$

Where, K_p, K_v, and K_i are the gain matrices of proportional, derivative, and integral control. In addition, ε, e, and $\dot{e}$ are the error functions of displacement, velocity, and acceleration. Moreover, q, $\dot{q}$, and $\ddot{q}$ are the position, rotational speed, and angular acceleration of the end-effector. M is the inertia tensor and τ is the torque.

According to Routh's test law and the decoupling of gain matrices, to maintain the stability of the system, there must be a relationship of 3.

$$K_{i_i} < K_{v_i} K_{p_i} \tag{3}$$

For example, with the help of the PID method, the path of the letter D has been controlled, which will be explained in the following. The letter D consists of a line segment and a curve. Figure 7 shows the PID controller Block Diagram operated in Simulink software.

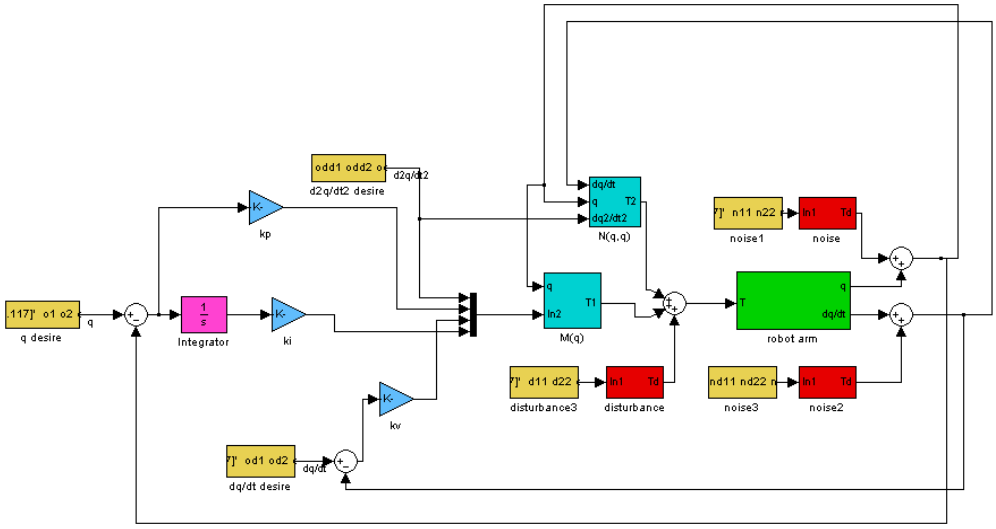

Figure 7. PID controller Block Diagram

In the block diagram, the robot arm is the controlled unit that consists of components such as motors, joints, parts, and sensors.

3. Results and Discussion

3.1 Robustness to Disturbance and Noise

Usually, the disturbance is modeled as an accumulative signal with the input torque signal to the robot. The amount of disturbance depends on environmental factors. External forces such as friction and the load of external objects imposed on the robot can cause non-structural uncertainty in the system, which is usually considered an input disturbance. The disturbance function may have various forms, but usually, to test the system, it is considered a step or sinusoidal function. The step function is used when a singular perturbation (in a very short time) affects the system and then disappears such as an impact by an external force. On the other hand, the sinusoidal function follows the system for a long period. For example, the heavy vibration of other industrial machines in the factory. In this article, both types of these functions are included in the disturbance and the results related to the sinusoidal function are shown. The perturbation ranges of the sine function for joints 1 to 5 are considered equal to 5, 60, 20, 0.5, and 0.1, respectively.

Often, noise is introduced in the form of measured noise added to the output in feedback (sensors). In most cases, the noise function is entered as a random or sinusoidal function. Of course, the

frequency of the noise function is considered much higher than the frequency of the disturbance function. The amplitude of the noise input to the feedback is considered to be about 0.001. The diagram of the path traveled by the end-effector before and after introducing disturbance and noise to the system is shown in Figure 8.

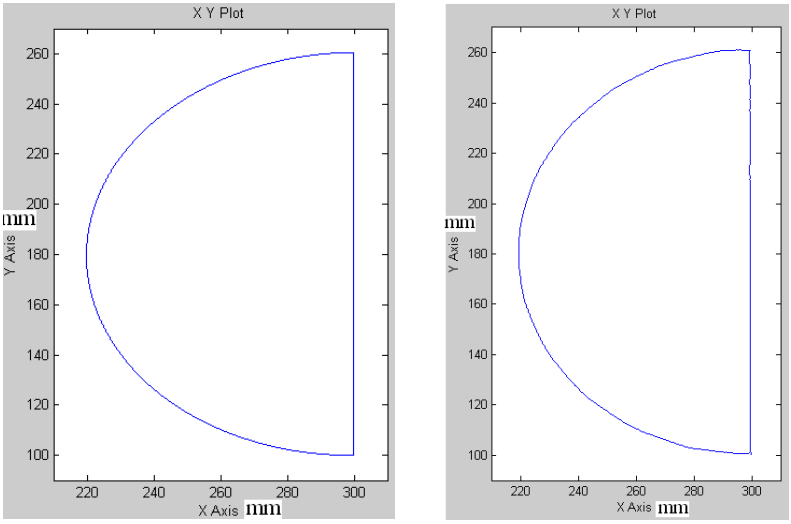

(a) (b)

Figure 8. Diagram of the path traveled by the end-effector (a) before and (b) after introducing disturbance and noise to the system

As shown in Figure 8 (b), there is a little shake can be observed on the path due to noise and disturbance, however, the final form of the letter D is acceptable and legible.

The error diagram of the trajectory (e) and the error diagram of velocity (ė) for five joints of the robot, before and after imposing the noise and disturbance, are shown in Figure 9 and Figure 10 respectively.

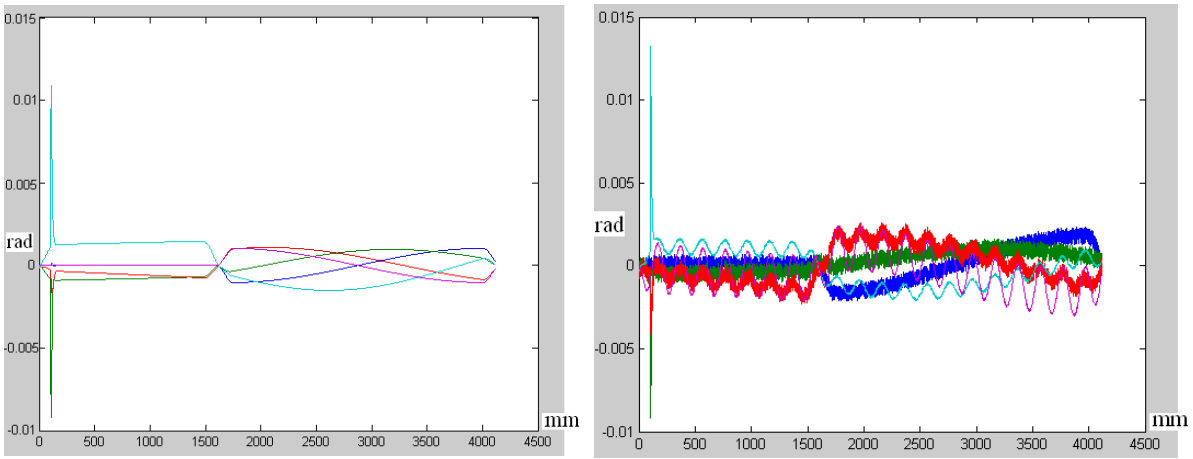

(a) (b)

Figure 9. Error diagram of the trajectory (e) for five robot joints (a) before and (b) after introducing disturbance and noise to the system

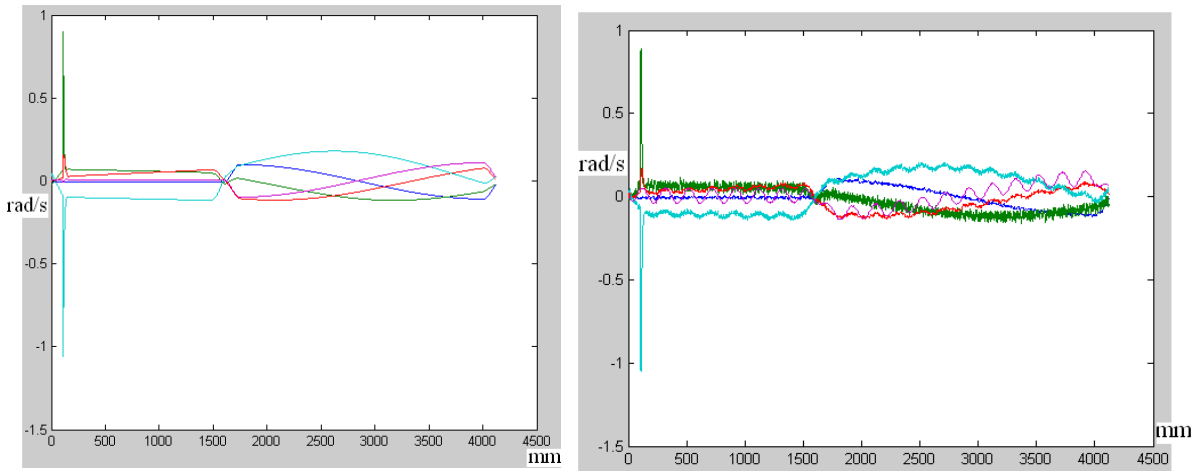

(a) (b)

Figure 10. Velocity error diagram (e•) for five robot joints (a) before and (b) after introducing disturbance and noise to the system

According to the error graphs, it can be said that the controller is not resistant to noise. The reason for that is the large gain value. The diagram of position and angular velocity (q and q•) for five joints of the robot despite disturbance and noise is shown in Figure 11 (a and b).

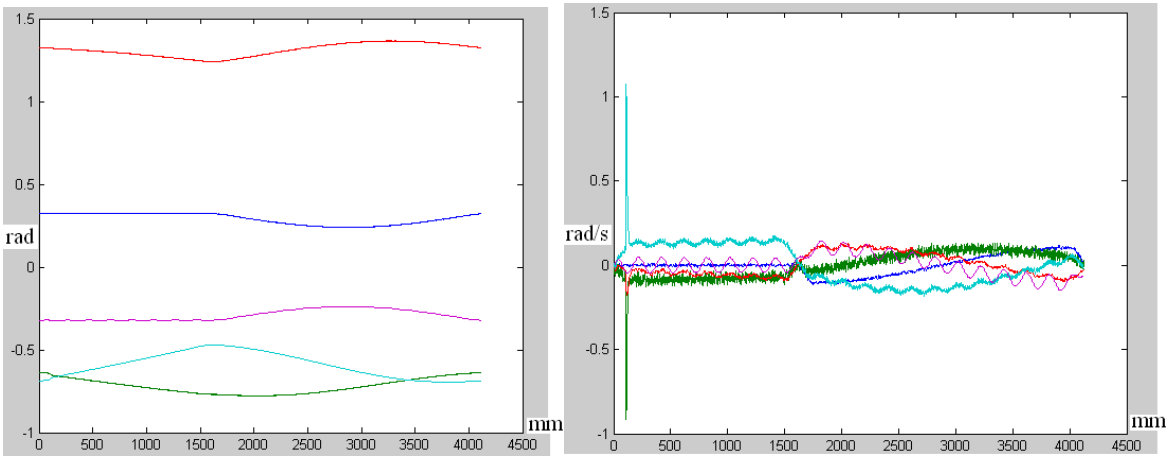

(a) (b)

Figure 11. (a) Position diagram (q) for five robot joints with disturbance and noise (b) Angular velocity diagram (q•) for five robot joints with presence of disturbance and noise

From the comparison of Figures 11 (a and b), it can be seen that noise and disturbance are more visible in the angular velocity diagram.

3.2 Investigating the performance of the robot in terms of crossing singular points

Singular points refer to points where Jacobian joints are not reversible. There are two ways to determine the Jacobi and, as a result, the singular points: 1- Using the method of Velocity Propagation between the links according to relations 4, it is possible to calculate the Jacobi [26]:

$$
\begin{aligned}
&{}^{i+1}v_{i+1} = {}^{i+1}R_i({}^{i}v_i + {}^{i}\omega_i \times {}^{i}P_{i+1}) \\
&{}^{i+1}\omega_{i+1} = {}^{i+1}R_i\,{}^{i}\omega_i + \dot{\theta}_{i+1}\,{}^{i+1}e_{i+1} \\
&{}^{EE}t_{EE} = \begin{bmatrix} {}^{E}\omega_E \\ {}^{E}v_E \end{bmatrix} \Longrightarrow \ {}^{EE}t_{EE} = {}^{EE}J\dot{q} \\
&{}^{0}J = \begin{bmatrix} {}^{0}R_E & 0 \\ 0 & {}^{0}R_E \end{bmatrix} {}^{EE}J
\end{aligned}
\tag{4}
$$

Where ω is rotational speed, *V* is linear velocity, *R* is the position vector, *J* is the Jacobian, *t* is the transfer matrix and *P* is the position vector from the center of the mass of the link.

2- Jacobi can be calculated with the help of *Screw Analysis*. To use this method, equation 5 should be applied [4].

$$
\begin{aligned}
&t_{EE} = {}^{EE}J\dot{q} \\
&t_{EE} = \begin{bmatrix} e_1 & e_2 & \dots & e_n \\ r_1 \times e_1 & r_2 \times e_2 & \dots & r_n \times e_n \end{bmatrix} \dot{q}
\end{aligned}
\tag{5}
$$

Where *J* is Jacobian, $\dot{q}$ is the velocity of the end-effector, and vector *r* is the position vector of the end-effector from the base of the robot.

In this article, both methods are used to calculate the Jacobi matrix and its determinants, and the singular points of the robot's path are determined (the results obtained from both methods are completely similar to each other). Figure 12 shows the determinant diagram of the Jacobi matrix along the path of the robot. As it is clear from Figure 12, along the path, the determinant of the Jacobi matrix does not become zero, or in other words, the robot does not pass its singular point.

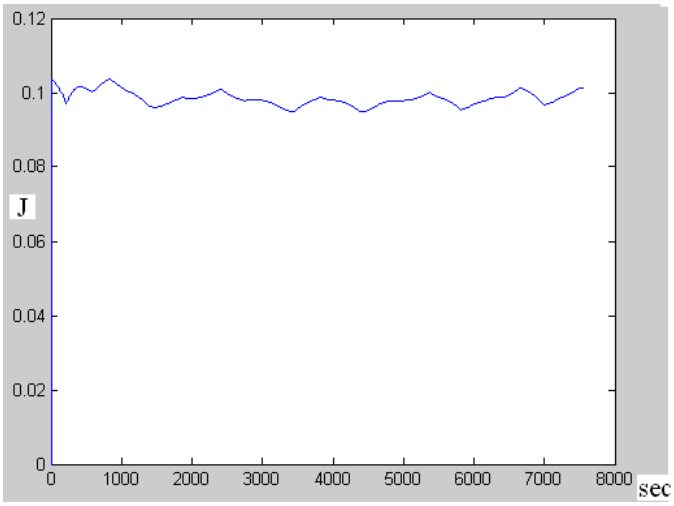

Figure 12- Diagram of the determinant of the Jacobi matrix along the path of the robot

4. Conclusions

In this article, the goal was to design a suitable controller for the marker robot to write on steel slabs. The conclusions are as follows:

- To design the controller, the dynamic equations of the robot must be obtained first. To obtain the dynamic equations of the robot, the end-effector path of the robot must first be designed. Therefore, the design of the path for writing letters and numbers was done and the dynamic equations of the robot were obtained by the Newton-Euler method.
- The control of the robot was done by the torque method calculated by using PID in the outer loop. The designed controller is resistant to disturbances, although it is less resistant to noise. The final performer of the robot travels the designed path suitably so that the words written by the final performer of the robot are readable despite the disturbance and noise.
- The passing of the robot from its singular point was checked and it was determined that the robot did not pass the singular point.

5. Acknowledgment

We are grateful to the Research Council of Shahid Chamran University of Ahvaz for financial support (SCU.EM1403.39184).

6. References

[1] Goel, R. and Gupta, P. 2020. Robotics and industry. A Roadmap to Industry 4.0, Smart Production, Sharp Business and Sustainable Development. Springer-IEREK, 157-169. doi: 10.1007/978-3-030-14544-6.

[2] Day, C.-P. 2018. Robotics in the industry-their role in intelligent manufacturing. Engineering. 4(4): 440-445. doi: 10.1016/j.eng.2018.07.012.

[3] Bragança, S., Costa, E. and Castellucci, I. and Arezes, P.M. 2019. Occupational and Environmental Safety and Health. A brief overview of the use of collaborative robots in industry 4.0: Human role and safety. Springer. doi: 10.1007/978-3-030-14730-368.

[4] Tantawi, K.H., Sokolov, A. and Tantawi, O. 2019. Advances in industrial robotics: From industry 3.0 automation to industry 4.0 collaboration. Proceedings of 4th Technology Innovation Management and Engineering Science International Conference (TIMES-iCON). doi:10.1109/TIMES-iCON47539.2019.9024658.

[5] Javaid, M., Haleem, A., Singh, R.P. and Suman, R. 2021. Substantial capabilities of robotics in enhancing industry 4.0 implementation. Cognitive Robotics. 1(1): 58-75. doi: 10.1016/j.cogr.2021.06.001.

[6] Kerber, E., Heimig, T., Stumm, S., Oster, L., Brell-Cokcan, S. and Reisgen, U. 2018. Towards robotic fabrication in joining of steel. Proc. ISARC. Proceedings of the International Symposium on Automation and Robotics in Construction. doi: 10.22260/ISARC2018/0062.

[7] Hollerbach, J.M. 1979. Understanding Manipulator Control by Synthesizing Human Handwriting. Springer.

[8] Suh, S.-H., Lee, J.-J., Choi, Y. J. and Lee, S. K. 1993. A prototype integrated robotic painting system: Software and hardware development. Proceedings of 1993 IEEE/RSJ International Conference on Intelligent Robots and Systems (IROS'93). doi:10.1109/IROS.1993.583145.

[9] Antonio, J.K. 1994. Optimal trajectory planning for spray coating. Proceedings of the IEEE international conference on robotics and automation. doi: 10.1109/ROBOT.1994.351125.

[10] Asakawa, N. and Takeuchi, Y. 1997. Teachingless spray-painting of sculptured surfaces by an industrial robot. Proc. Proceedings of international conference on robotics and automation. doi: 10.1109/ROBOT.1997.619061.

[11] Hertling, P., Hog, L., Larsen, R., Perram, J.W. and Petersen, H.G. 1996. Task curve planning for painting robots. I. Process modeling and calibration. IEEE Transactions on Robotics and Automation. 12(2): 324-330. doi: 10.1109/70.488951.

[12] Mahdieh, M.S. 2023. Improving surface integrity of electrical discharge machined ultra-fined grain al-2017 by applying rc-type generator. Proceedings of the Institution of Mechanical Engineers. Part E: Journal of Process Mechanical Engineering. 1(1): 1-9. doi: 10.1177/09544089231202329.

[13] Mahdieh, M.S. and Esteki, M.R. 2022. Feasibility investigation of hydroforming of dental drill body by fem simulation. Journal of Modern Processes in Manufacturing and Production. 11(2): 71-83. doi: 20.1001.1.27170314.2022.11.2.7.5

[14] Mahdieh, M.S. and Monjezi, A. 2022. Investigation of an innovative cleaning method for the vertical oil storage tank by fem simulation. Iranian Journal of Materials Forming. 9(4): 5-12. doi: 10.22099/ijmf.2022.43842.1229

[15] Mahdieh, M.S., Nazari, F., Mussa, T.A. and Salehi, H.T. 2023. A study on stamping of airliner's tail connector part through fem simulation. Journal of Simulation and Analysis of Novel Technologies in Mechanical Engineering. 15(3): 5-13.

[16] Mahdieh, M.S., Zadeh, H.M.B. and Reisabadi, A.Z. 2023. Improving surface roughness in barrel finishing process using supervised machine learning. Journal of Simulation and Analysis of Novel Technologies in Mechanical Engineering. 15(2): 5-15. doi: 20.1001.1.27834441.2023.15.2.1.0.

[17] Mahdieh, M. S., Nazari, F. and Khairullah, A.R. 2024. A study on the effects of different pad materials on brake system performance of a high-capacity elevator by fem simulation. International Journal of Advanced Design and Manufacturing Technology. 65(4): 61-68. doi: 10.30486/ADMT.2023.873808.

[18] Vakili Sohrforozani, A., Farahnakian, M., Mahdieh, M.S., Behagh, A.M. and Behagh, O. 2019. A study of abrasive media effect on deburring in barrel finishing process. Journal of Modern Processes in Manufacturing and Production. 8(3): 27-39. doi:10.30495/ADMT.2020.1889912.1165.

[19] Vakili Sohrforozani, A., Farahnakian, M., Mahdieh, M.S., Behagh, A.M. and Behagh, O. 2020. Effects of abrasive media on surface roughness in barrel finishing process. ADMT Journal. 13(3): 75-82. doi:10.30495/ADMT.2020.1889912.1165.

[20] Foley, F., O'Donoghue, C. and Walsh, J. 2023. Optimizing the implementation of a robotic welding system. Journal of Modern Processes in Manufacturing and Production. 12(2): 39-52. dor: 20.1001.1.27170314.2023.12.2.3.8.

[21] Hasanabadi, A. 2022. Path optimization of moving object in presence of obstacles using messy genetic algorithm for n-dimensional space. Journal of Modern Processes in Manufacturing and Production. 11(3): 51-60. dor: 20.1001.1.27170314.2022.11.3.5.5.

[22] Deylami, A. 2021. Stability of robust lyapunov based control of flexible-joint robots using voltage control strategy revisited. Journal of Modern Processes in Manufacturing and Production. 10(4): 13-25. dor: 20.1001.1.27170314.2021.10.4.1.6.

[23] Mallahi Kolahi, P. and Mosayebi, M. 2021. Optimal trajectory planning for an industrial mobile robot using optimal control theory. Journal of Modern Processes in Manufacturing and Production. 10(3): 25-34. dor: 20.1001.1.27170314.2021.10.3.4.7.

[24] Deylami, A. 2021. Tracking control of robots revisited based on taylor series and asymptotic expansion. Journal of Modern Processes in Manufacturing and Production. 10(2): 63-70. dor: 20.1001.1.27170314.2021.10.2.6.7.

[25] Moshayedi, A.J., Xu, G., Liao, L. and Kolahdooz, A. 2021. Gentle survey on mir industrial service robots: Review & design. Journal of Modern Processes in Manufacturing and Production. 10(1): 31-50. dor: 20.1001.1.27170314.2021.10.1.3.2.

[26] Craig, J.J. 2006. Introduction to Robotics: Mechanics and Control, 4th edition, Pearson.

[27] Westervelt, E.R., Grizzle, J.W., Chevallereau, C., Choi, J.H. and Morris, B. 2018. Feedback Control of Dynamic Bipedal Robot Locomotion. CRC Press. doi: 10.1109/TAC.2008.918096.